THE JOURNAL OF BIOLOGICAL CHEMISTRY VOL. 281, NO. 47, pp. 36044–36051, November 24, 2006

Nephrocan, a Novel Member of the Small Leucine-rich Repeat Protein Family, Is an Inhibitor of Transforming Growth Factor-β Signaling*

Received for publication, May 18, 2006, and in revised form, August 29, 2006 Published, JBC Papers in Press, September 21, 2006, DOI 10.1074/jbc.M604787200

Yoshiyuki Mochida[‡], Duenpim Parisuthiman[‡], Masaru Kaku[‡], Jun-ichi Hanai[§], Vikas P. Sukhatme[§], and Mitsuo Yamauchi[‡1]

From the [‡]Dental Research Center, University of North Carolina, Chapel Hill, North Carolina 27599-7455 and [§]Divisions of Nephrology and Hematology-Oncology, Departments of Medicine and Pathology, Center for Study of the Tumor Microenvironment, Beth Israel Deaconess Medical Center, Harvard Medical School, Boston, Massachusetts 02215

In a search of new, small leucine-rich repeat proteoglycan/protein (SLRP) family members, a novel gene, nephrocan (NPN), has been identified. The gene consists of three exons, and based on the deduced amino acid sequence, NPN has 17 leucine-rich repeat motifs and unique cysteine-rich clusters both in the N and C termini, indicating that this gene belongs to a new class of SLRP family. NPN mRNA was predominantly expressed in kidney in adult mice, and during mouse embryogenesis, the expression was markedly increased in 11-day-old embryos at a time when early kidney development takes place. In the adult mouse kidney, NPN protein was located in distal tubules and collecting ducts. When NPN was overexpressed in cell culture, the protein was detected in the cultured medium, and upon treatment with *N*-glycosidase F, the molecular mass was lowered by ~14 kDa, indicating that NPN is a secreted *N*-glycosylated protein. Furthermore, transforming growth factor-β (TGF-β)-responsive 3TP promoter luciferase activity was down-regulated, and TGF-β-induced Smad3 phosphorylation was also inhibited by NPN, suggesting that NPN suppresses TGF-β/Smad signaling. Taken together, NPN is a novel member of the SLRP family that may play important roles in kidney development and pathophysiology by functioning as an endogenous inhibitor of TGF-β signaling.

Leucine-rich repeat (LRR)[2] is a highly conserved motif from bacteria to mammals, and LRR proteins have diverse structural, biological, and cellular functions such as matrix organization, host defense, inflammation, and cell death (1–3). LRR is composed of 20–29 amino acid residues rich in hydrophobic amino acids such as leucine, isoleucine, and valine. Recently, the three-dimensional structures of several LRR proteins such as human ribonuclease inhibitor, light chain1 of dynein, plague virulence protein, YopM, etc. have been determined (4–6), and all of the structures reported have significant similarities forming a curved shape with a parallel β-sheet on the concave side and helical elements primarily on the convex side. This specific structure has been thought to be a conformation ideal for binding to other proteins (5). In addition, recent structural studies on LRR proteins support the characteristic horseshoe structure (7, 8) with more variations (9).

Small leucine-rich proteoglycans/proteins (SLRPs) are an evolutionally conserved family of secreted proteins that are synthesized as a small core protein containing 6–20 LRR motifs and post-translationally modified with glycosaminoglycan chain(s), *N*-glycosylation, and/or tyrosine sulfation (10). It has been suggested that SLRP family members play important roles in collagen fibrillogenesis, cellular proliferation, cell differentiation, and migration in various tissues (11, 12). They are divided into several subclasses depending on numbers of exons, interspaced amino acids within the N-terminal cysteine cluster, and LRR motifs. Decorin (DCN), a prototype member of the SLRP family, belongs to class I and is composed of a characteristic N-terminal cysteine cluster (CX_3CXCX_6C), a central region containing 10 LRR motifs, and a C-terminal cysteine cluster. DCN is ubiquitously expressed, and it has been extensively characterized as a collagen-binding protein (13–17) modulating collagen fibrillogenesis (18, 19). DCN has also been shown to inhibit cell growth as a putative tumor suppressor (20, 21) and to bind to transforming growth factor-β (TGF-β) as a regulator of growth factor functions (22, 23). At present, 15 SLRP members have been cloned and partially characterized, and most are located in clusters on human and mouse chromosome (24).

Here we present a new member of the SLRP family identified by a bioinformatics approach using DCN as a query protein sequence. Because this protein appears to be specifically expressed in kidney, it is named as "nephrocan (NPN)". Its gene structure, mRNA expression pattern, distribution, cellular

* This work was supported by National Institutes of Health Grants NIDCR-DE10489 (to M. Y.) and NIAMS AR052824 (to M. Y.) and NASA Grant NAG2-1596 (to M. Y.). The costs of publication of this article were defrayed in part by the payment of page charges. This article must therefore be hereby marked "*advertisement*" in accordance with 18 U.S.C. Section 1734 solely to indicate this fact.

The nucleotide sequence(s) reported in this paper has been submitted to the GenBank™/EBI Data Bank with accession number(s) AY938536, DQ233647, and DQ166815.

[1] To whom correspondence should be addressed: CB 7455, Dental Research Center, University of North Carolina, Chapel Hill, NC 27599-7455. Tel.: 919-966-3441; Fax: 919-966-1231; E-mail: Mitsuo_Yamauchi@dentistry.unc.edu.

[2] The abbreviations used are: LRR, leucine-rich repeat; SLRPs, small leucine-rich proteoglycans/proteins; DCN, decorin; TGF-β, transforming growth factor-β; NPN, nephrocan; EST, expressed sequence tags; RT, reverse transcription; HA, hemagglutinin; GAPDH, glyceraldehyde-3-phosphate dehydrogenase; PBS, phosphate-buffered saline; PVDF, polyvinylidene fluoride; CS, chondroitin sulfate; DS, dermatan sulfate; EMT, epithelial-mesenchymal transition; MET, mesenchymal-epithelial transition; LAP, latency-associated peptide; WB, Western blotting.

localization, effects on TGF-β activity, and potential functions are described in this study.

EXPERIMENTAL PROCEDURES

Cell Culture—Human embryonic kidney 293 cells were purchased from Clontech and maintained in Dulbecco's modified Eagle's medium (Invitrogen) containing a high concentration of glucose (4.5 mg/ml), supplemented with 10% fetal bovine serum (Sigma), 100 units/ml penicillin, and 100 μg/ml streptomycin in a 5% CO_2 atmosphere at 37 °C.

Molecular Cloning of Mouse Nephrocan cDNA—To identify a new member of the SLRP family, we first obtained the oreochromis niloticus (nile tilapia) ortholog of DCN (GenBank™ accession number; AF247822) as a query protein sequence and performed a BLAST search of the mouse genome. The candidate sequences were then obtained, and the PSORT II program was used to predict the subcellular localization. This computational screening identified a probable extracellular molecule, NPN, that has a signal peptide sequence but lacks a transmembrane domain. Next we searched its tissue distribution based on the expressed sequence tags (EST) data base sequences. According to that computational information, NPN mRNA was expressed in kidney (EST sequence numbers CA468708.1, AW611331.1, and BX512695.1), aorta (BB224812.1 and BB223005.1), pancreas (BM055738.1), and 8-day-old embryos (AV311419.1). The cDNA derived from kidney was therefore used as a template. The cDNAs containing the coding sequence of NPN were isolated by RT-PCR using Hotstar TaqDNA polymerase (Qiagen). The sequences of the primers were as follows: forward primer, 5′-GCAATGCACCCGCTTTGGGCTTTTC-3′, and reverse primer, 5′-ATCTATTTCATAATCGTCATCGTCGTC-3′. The PCR product was then ligated into the pcDNA3.1-V5/His-TOPO mammalian expression vector (Invitrogen), sequenced at the University of North Carolina at Chapel Hill, DNA Sequencing Facility, and the DNA sequence was 100% identical with the one deposited in the public source (NCBI reference sequence number NM_025684). The coding sequence of NPN was then subcloned into pcDNA3 fused with hemagglutinin (HA) tag vector (kindly provided by Dr. H. Ichijo, University of Tokyo, Japan) and the pcDNA3.1-V5/His-TOPO mammalian expression vector and sequenced (pcDNA3-NPN-HA and pcDNA3.1-NPN-V5/His). The sequences including 5′- and 3′-untranslated regions were also amplified with the forward primer, 5′-TGCTTGCTACTTGCAAAC-3′, and reverse primer, 5′-GCCTAAGTTTCAGACTAAAACACAAC-3′. The PCR product was ligated into pCR 2.1-TOPO vector (Invitrogen) and sequenced.

Tissue Distribution Determined by RT-PCR and Real Time PCR—RT-PCR was performed using the mouse MTC panel I (BD Biosciences) containing cDNA of heart, brain, spleen, lung, liver, skeletal muscle, kidney, testis, 7-, 11-, 15-, and 17-day-old embryo as templates. The sequences of primers for NPN were designed as follows: forward primer, 5′-CAGAATCTGCTGTTGTCTATCCCTC-3′ and reverse primer, 5′-CACACTTGTGCTTAAGACAGTGGAC-3′. RT-PCR using glyceraldehyde-3-phosphate dehydrogenase (GAPDH) control primers provided with the MTC panel I was also performed with the same templates. The PCR conditions were as follows: 15 min at 95 °C, 30 s at 95 °C, and 3 min at 68 °C for 38 cycles (NPN) or for 22 cycles (GAPDH). The PCR products amplified by NPN or by GAPDH primers were analyzed on a 1.2% agarose gel.

To quantitatively analyze the expression levels of NPN, aliquots of cDNA of mouse MTC panel I were also used as templates for NPN (ABI assay number Mm00481816_m1) or GAPDH (ABI assay number 4308313). Real time PCR was performed in triplicate using the ABI Prism 7000 sequence detection system (Applied Biosystems). The mean fold changes in the expression of NPN relative to that of GAPDH were calculated using the values of the expression of either mouse heart or 7-day-old embryo cDNA as a calibrator by means of $2^{-\Delta\Delta C_T}$ method as described previously (25).

Generation and Characterization of Anti-NPN Antibody—A polyclonal NPN antibody was generated by immunizing rabbits with a synthetic peptide corresponding to the sequence in the 4th LRR region of NPN, *i.e.* ^{112}SALPANLEVLKLNDNAIC^{129} (Alpha Diagnostic International Inc., San Antonio, TX). Both preimmune serum and anti-NPN polyclonal antibody were then further affinity-purified with ImmunoPure (A Plus) IgG purification kit (Pierce) and used for Western blot analyses. The heart, lung, liver, brain, and kidney tissues obtained from Harlan Sprague-Dawley mice (8–12 weeks) were pulverized and then extracted with 6 M guanidine-HCl, pH 7.4, for 2 days at 4 °C, and the supernatants were separated from the insoluble residues by centrifugation (15,000 × *g*) for 30 min, dialyzed against distilled water, and lyophilized. Aliquots of dried samples were dissolved in lysis buffer containing 150 mM NaCl, 20 mM Tris-HCl, pH 7.5, 10 mM EDTA, 1% Triton X-100, 1% sodium deoxycholate, 1.5% aprotinin, and 1 mM phenylmethylsulfonyl fluoride and centrifuged, and the protein concentrations in the supernatants were measured by a platereader using a DC protein assay kit (Bio-Rad). The samples with equal amounts of proteins were then subjected to Western blot analysis with anti-NPN antibody, preimmune serum, or anti-V5 antibody (Invitrogen) as described below.

Purification of NPN-V5/His Fusion Protein—pcDNA3.1-NPN-V5/His vector was transfected into 293 cells using FuGENE 6 transfection reagent (Roche Diagnostics) according to the manufacturer's instructions, and the cells were cultured in the presence of 400 μg/ml of G418 (Invitrogen) for 3–4 weeks to select stably transfected clones. Positive clones derived from G418-resistant cells were then isolated by cloning rings and further grown in the same conditions. Equal numbers of cells in each clone were plated onto 6-well culture plates at a density of 3×10^5cells/well and cultured for 3 days. Cultured media were then collected and subjected to Western blot analyses with anti-V5 antibody to assess the NPN-V5/His protein levels synthesized by the clones. The clone that synthesized the highest level of NPN-V5/His protein was further cultured for 6 days, and the cultured medium was collected. NPN-V5/His fusion protein was purified using a nickel-nitrilotriacetic acid-agarose resin (Qiagen), and purified proteins were pooled, dialyzed against distilled water, lyophilized, and kept at −20 °C until use. To determine the purity of NPN-V5/His protein, aliquots of the dried samples were dissolved in distilled water, and protein concentration was measured using a DC protein assay kit (~50 ng/μl), solubilized in SDS sample buffer (100 mM Tris-

HCl, pH 8.8, 0.01% bromphenol blue, 36% glycerol, 4% SDS) in the presence of 10 mM dithiothreitol, and separated by 4–12% SDS-PAGE. The samples were analyzed by Coomassie Brilliant Blue R-250 staining and Western blotting using anti-NPN antibody or anti-V5 antibody as described below.

Immunohistochemistry—To determine the distribution of NPN within kidney, immunohistochemical staining was performed using Vectastain Elite ABC kit (Vector Laboratories Inc.). Formalin-fixed paraffin-embedded sections of nondiseased control adult mouse kidney or liver were deparaffinized with xylene and graded ethanol and treated with 20 μg/ml proteinase K (Roche Diagnostics) for 10 min. The sections were then incubated with 0.3% H_2O_2 in methanol for 30 min, followed by incubation with anti-NPN antibody (diluted in 1:200) overnight at 4 °C. After washing with phosphate-buffered saline (PBS) several times, sections were further incubated with biotinylated IgG for 20 min and subsequently with avidin and biotinylated horseradish peroxidase for 20 min. Following several washes with PBS, 3,3′- diaminobenzidine nickel substrate (Vector Laboratories Inc.) was applied, and the sections were also counterstained with hematoxylin (Sigma).

To verify the specificity of the anti-NPN antibody, the effect of the synthetic peptide used for immunization on the immunoreactivity was evaluated. The anti-NPN antibody with or without the synthetic peptide was incubated overnight at 4 °C and subjected to immunostaining in the same manner as describe above. Purified preimmune serum described above was used as a negative control. The immunoreactivities of specimens visualized were photographed under a light microscope (Nikon-FXA) at a magnification of ×20.

Immunoprecipitation and Western Blot Analysis—To examine the subcellular localization of NPN, 293 cells were plated onto 6-well culture plates at a density of 3×10^5 cells/well, and on the following day, the cells were transfected with an empty pcDNA3.1-V5/His A vector (Invitrogen) or pcDNA3.1-NPN-V5/His vector using FuGENE 6 transfection reagent. After 72 h, the cultured medium was collected, and the transfected cells were washed with PBS and lysed with the lysis buffer. The cultured medium and the lysate were then incubated with anti-V5 antibody. After addition of protein A-Sepharose 4B conjugate (Zymed Laboratories Inc.), the samples were incubated for an additional 30 min, and the beads were washed twice with the lysis buffer, solubilized in SDS sample buffer in the presence of 10 mM dithiothreitol, and separated by 4–12% SDS-PAGE. The proteins were transferred to a polyvinylidene fluoride membrane (Immobilon-P; Millipore), reacted with anti-V5 antibody, and detected by alkaline phosphatase conjugate substrate kit (Bio-Rad). As for Smad3 phosphorylation, 293 cells were treated with 10 ng/ml of human TGF-β1 (R&D Systems) with or without purified NPN-V5/His fusion protein and incubated for 24 h. Cell lysate was used for Western blotting with anti-phospho-Smad3 antibody (BIOSOURCE). Equal protein loading was confirmed using anti-actin antibody (Sigma). Three independent experiments were performed, and the results were essentially identical.

N-Glycosylation Analysis—To examine whether or not NPN is *N*-glycosylated, 293 cells were plated onto 6-well culture plates at a density of 3×10^5 cells/well and transfected with the pcDNA3.1-NPN-V5/His vector. After 72 h, the cultured medium was immunoprecipitated with anti-V5 antibody, and the immunocomplex was collected using protein A-Sepharose beads. Aliquots of the samples were then treated with *N*-glycosidase F enzyme (Prozyme Inc., San Leandro, CA) for 24 h at 37 °C, subjected to Western blot analysis in the same manner as described above, and compared with the untreated samples.

Luciferase Assay—293 cells were transiently transfected with a combination of the following vectors: 3TP luciferase reporter plasmid vector, *Renilla* expression vector pRL-TK, NPN expression vectors (pcDNA3-NPN-HA or pcDNA3.1-NPN-V5/His). Cells were treated with 10 ng/ml human TGF-β1, and the luciferase activities in the cell lysates were determined using the dual reporter assay system (Promega). The firefly luciferase activities were then normalized to the *Renilla* luciferase activities under the control of thymidine kinase promoter. Furthermore, after the transfection of 3TP luciferase and *Renilla* vectors, TGF-β1 was added together with purified NPN-V5/His fusion protein (~50 ng/μl), and the luciferase activities were measured in the same manner. All of the luciferase experiments were performed in triplicate.

RESULTS

NPN Belongs to a New Class of the SLRP Family—Based on the predicted amino acid sequences, NPN is a 512-amino acid-long protein and shares some structural characteristics with other SLRP members, *i.e.* it has a putative signal peptide sequence, a characteristic cysteine cluster (CX_3CXCX_7C) in the N terminus (Fig. 1*A*), 17 LRR motifs (Fig. 1*B*), and 3 exons (Fig. 1*C*). However, NPN has several features distinct from other SLRP members, including four cysteine residues in the C-terminal flanking domain, five potential *N*-glycosylation sites, and a polyacidic amino acid tail (DDDDDDYEID) at the C terminus (Fig. 1*A*). Characterization of the LRR motif was based on the general consensus sequence (2, 26, 27) for type T (*zzxx-axxxx*F*xxaxx*L*xx*L*x*L*xx*N*x*L) and type S (*xxa*P*zx*LP*xx*L*xx*L*x*-L*xx*N*xI*). In both types of LRR motifs, "*z*" is frequently a gap; "*x*" indicates variable residues; "*a*" is valine, leucine, or isoleucine; and *I* is isoleucine or leucine. In NPN, of 17 LRR motifs, there are 11 type T and 6 type S present (Fig. 1*B*). Based on these criteria (27), class I and II SLRPs have 12 LRR motifs composed of four tandem STT "super-motifs,", *i.e.* $(STT)_4$. Class III SLRPs, including epiphycan and osteoglycin, have 7 LRRs composed of $(ST)T(ST)_2$. Chondroadherin, a representative of class IV member, contains 10 type T LRRs. Although the conserved asparagine residues of LRR1 and LRR2 in NPN are substituted with serine (LRR1) and glutamic acid (LRR2), the organization of LRRs in NPN is unique, *i.e.* $(STT)_2ST(STT)_3$. The NPN gene is localized on mouse chromosome locus 10 *in silico* and spans over 1.4 kbp (Fig. 1*C*). Phylogenetic tree analysis of NPN together with the known SLRP members was performed using the ClustalW server and ClustalX program (28) (Fig. 1*D*). The mouse protein sequences used in this study were obtained from the public data base deposited as NCBI reference sequences. These results indicate that NPN belongs to a new class of the SLRP family (2, 10, 12, 26, 27).

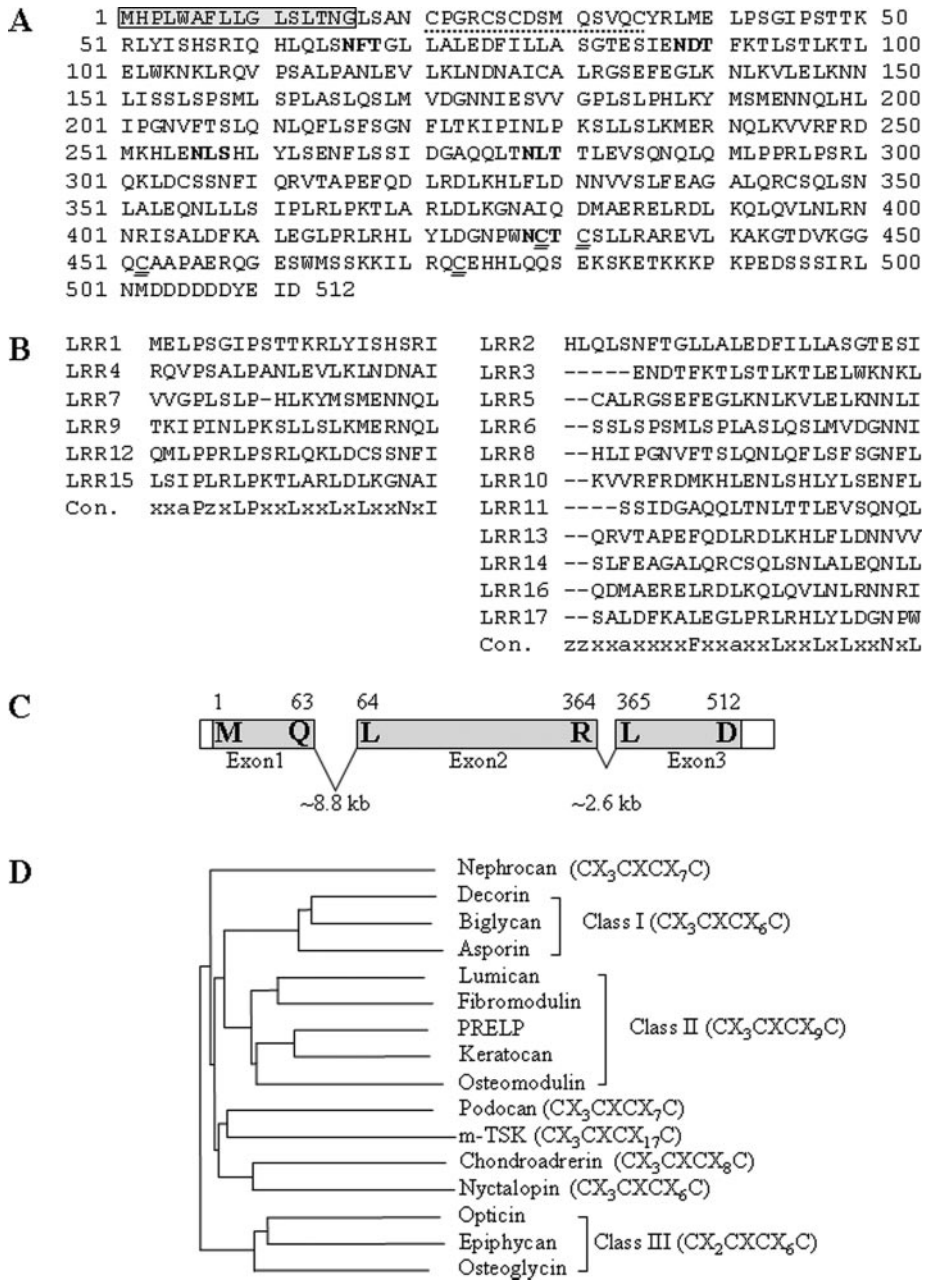

FIGURE 1. **The amino acid sequence, gene structure, and phylogenetic analysis of nephrocan.** *A,* the deduced amino acid sequence of NPN. The putative signal peptide sequence and cleavage site (*boxed in gray*) were predicted using the PSORT II program. Potential *N*-glycosylation sites (N*X*(S/T), where *X* is any amino acid) are in *boldface.* The N-terminal cysteine cluster (CX_3CXCX_7C, where C is cysteine, and *X* is any amino acid) is indicated by a *dotted underline* and C-terminal cysteine residues by *double underlines*. *B,* 17 LRR motifs aligned based on the ClustalW program. A consensus sequence (*Con.*) is displayed below the alignments. The LRR groups listed on the *left* represent type S LRR (*xxa*P*zx*L*Px*x*Lx*x*Lx*x*Nx*I*), and those on the right type T LRR (*zzxxaxxxx*F*xxaxx*L*xx*L*x*L*xx*NxL, where *x* is variable residue; *z* is frequently a gap; *a* is valine, leucine, or isoleucine; *P* is proline; *N* is asparatic acid; and *I* is isoleucine or leucine), respectively. *C,* the gene structure of NPN consisting of three exons. *D,* phylogenetic tree analysis of NPN together with other mouse SLRP members. PRELP is proline/arginine-rich end leucine-rich repeat protein; *m-TSK* is mouse ortholog of tsukushi (35).

Tissue Distribution of NPN—To determine the tissue distribution of NPN mRNA expression, both RT-PCR and real time PCR analyses were performed. As shown in Fig. 2*A*, the band amplified using NPN-specific primers was clearly detected in adult kidney and, to a much lesser extent, in heart, lung, and skeletal muscle. The expression was undetectable in all other tissues. Using the cDNA of mouse embryos at various stages, its expression was found to be transiently up-regulated at day 11 and decreased thereafter.

To quantify the levels of NPN mRNA expression among the tissues tested, real time PCR analysis was performed. The results also demonstrated that the expression level in kidney was the highest (~6-fold of that in heart) among the tissues tested in adult mice, and that during the embryonic development, the expression was highest at day 11 (~2-fold of that in embryonic day 7), a time critical for kidney development (29) (Fig. 2*B*). The results were further confirmed by analyzing another set of mouse MTC panel I (data not shown).

Localization of NPN Protein—To determine the tissue distribution of NPN protein, an anti-NPN antibody was generated, and its specificity was characterized. To confirm the NPN-V5/His protein was purified, the protein was stained by Coomassie Brilliant Blue R-250 (Fig. 3*A*, *lane 2*), and a single band was observed at the expected molecular weight size. The same protein was further analyzed by Western blotting using anti-NPN antibody and anti-V5 antibody (Fig. 3*A*, *lanes 1* and *3*), and it was immunoreactive to both antibodies. Because the epitope for the former resides in the N-terminal region of NPN, and the V5 tag was fused to the C terminus of NPN, these results demonstrate that the full-length NPN-V5/His protein was successfully purified (Fig. 3*A*) and that anti-NPN antibody recognizes NPN. The tissue distribution of NPN was then examined by Western blot analysis with this antibody using the protein lysates derived from heart, lung, liver, brain, and kidney. The purified NPN-V5/His fusion protein was used as a positive control. The results demonstrated that the endogenous NPN protein (an ~70-kDa band in Fig. 3*B*) was detected in kidney and, to a lesser extent, in heart and lung but not in liver and brain (Fig. 3*B*, *left panel, lanes 1–5*). The immunoreactive bands were observed as a doublet in kidney possibly because of the varied extent of post-translational modifications, the presence of a splicing variant, or protein processing/degradation (Fig. 3*B, left panel, lane 5*). This tissue distribution was

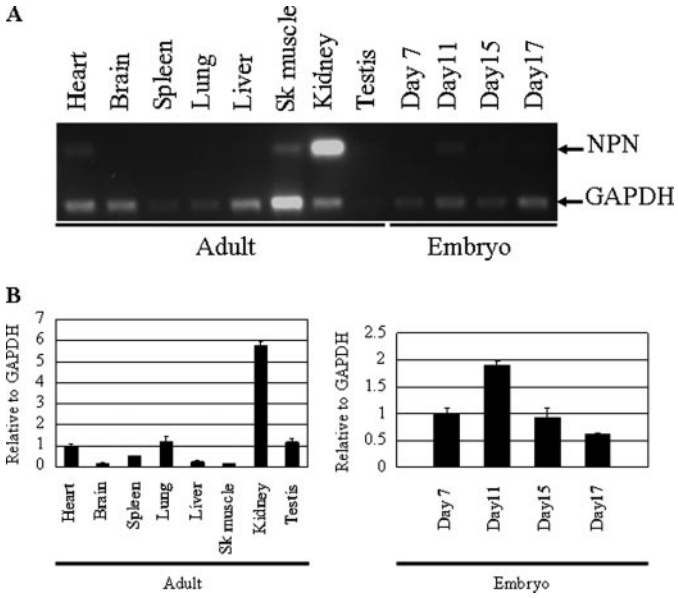

FIGURE 2. **Tissue distribution of NPN.** *A,* RT-PCR analysis with NPN-specific primers or glyceraldehyde-3-phosphate dehydrogenase (*GAPDH*)-specific primers was performed. The PCR products were analyzed on 1.2% TAE-agarose gel and photographed under UV light. *Sk muscle*, skeletal muscle. *B,* quantitative real time PCR analysis of NPN mRNA expression. The mean fold changes in the expression of NPN relative to that of GAPDH were calculated using the value of the expression of either heart or 7 day-embryo as a calibrator. The values are shown as mean ± S.D. based on triplicate assays. Sk muscle; skeletal muscle.

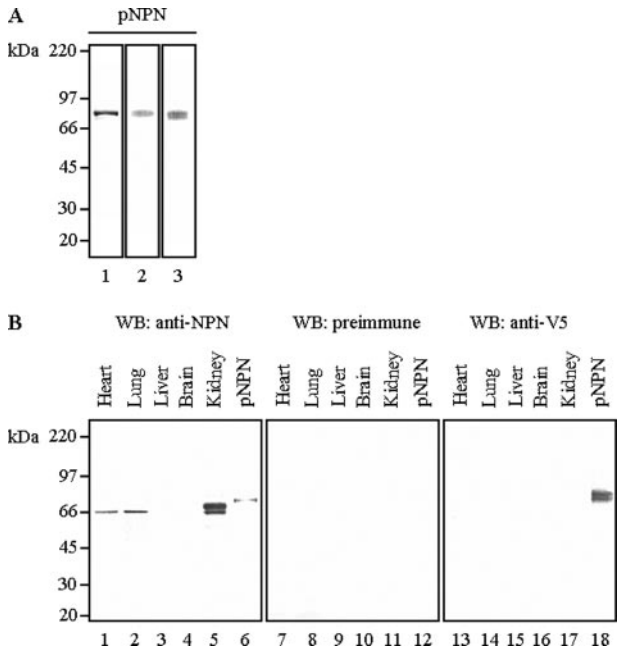

FIGURE 3. **Specificity of anti-NPN antibody (*A*) and distribution of NPN protein in mouse adult tissues (*B*).** *A,* purified NPN-V5/His fusion protein (pNPN) was subjected to Western blot analysis with anti-NPN antibody (*lane 1*) showing its immunoreactivity to pNPN. The purity of pNPN was verified by Coomassie Brilliant Blue R-250 staining (*lane 2*) and Western blot analysis with anti-V5 antibody (*lane 3*). The molecular weight of pNPN and its immunoreactivity to both antibodies indicate that pNPN is a full-length NPN. Markers of molecular mass are shown on the *left*. *B,* the proteins extracted from heart, lung, liver, brain and kidney tissues were analyzed by Western blotting (*WB*) with anti-NPN antibody (*left panel*), preimmune serum (*middle panel*), or anti-V5 antibody (*right panel*). NPN-V5/His fusion protein (pNPN) was used as a positive control. Markers of molecular mass are shown on the *left*.

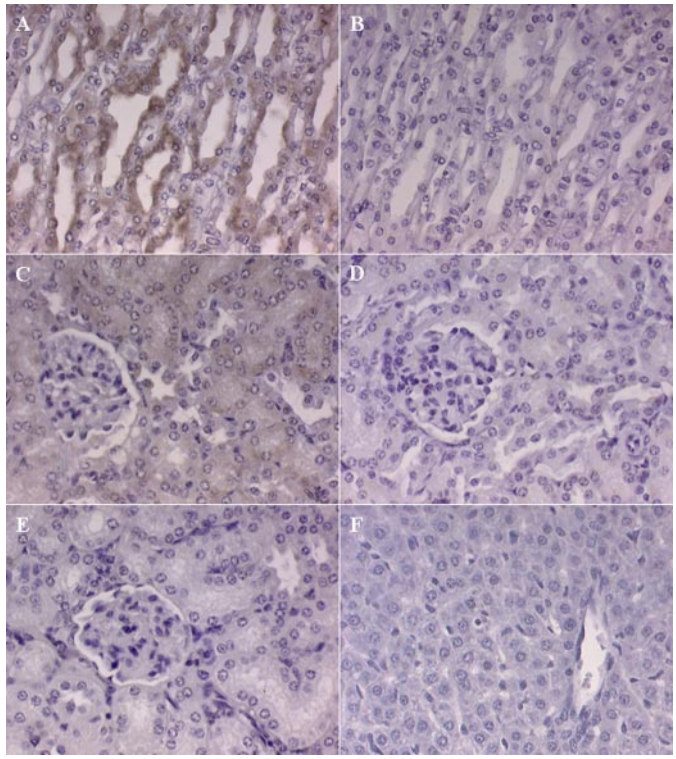

FIGURE 4. **Immunohistological detection of NPN in mouse adult kidney.** The mouse adult kidney sections were immunostained using anti-NPN antibody with (*B* and *D*) or without (*A* and *C*) the synthetic peptide used for antibody generation. The epithelial cells of distal tubules and collecting ducts were extensively stained (*A*), and proximal epithelial cells were slightly stained (*C*). There was no significant staining in glomeruli (*C*). The immunoreactivities were not observed using anti-NPN antibody in the presence of the synthetic peptide (*B* and *D*). Preimmune serum was also used as a negative control, and no immunoreactivities were observed (*E*). In liver, no immunoreactivities were observed (*F*). The specimens were observed and photographed under a light microscope at a magnification of ×20.

consistent with its mRNA expression pattern (Fig. 2). The purified NPN-V5/His fusion protein (pNPN) was detected at a slightly higher molecular weight position likely because of the presence of V5/His tag (~5 kDa) (Fig. 3*B*, *left panel, lane 6*). When Western blot analysis was done with either preimmune serum or anti-V5 antibody, there were no immunoreactive bands corresponding to the expected sizes in the tissue lysates (Fig. 3*B*, *middle panel, lanes 7–12,* and *right panel, lanes 13–17*). An intense immunoreactive band was detected for NPN-V5/His fusion protein when incubated with anti-V5 antibody (Fig. 3*B*, *right panel, lane 18*).

Using anti-NPN antibody we further examined the distribution of NPN protein in adult mouse kidney. As shown in Fig. 4, the epithelial cells, but not fibroblasts, of distal tubules and collecting ducts were extensively stained, and proximal epithelial cells were slightly stained. There was no significant staining in glomeruli (Fig. 4, *A* and *C*). In the presence of the synthetic peptide together with anti-NPN antibody, the structures described above were not immunostained, confirming the specific immunolocalization of NPN (Fig. 4, *B* and *D*). Preimmune serum was also used as a negative control, and no immunoreactivities were observed (Fig. 4*E*). No immunoreactivities were observed in liver where NPN gene expression was not detected (Fig. 4*F*).

NPN Is a Secreted Glycoprotein—Because many SLRP family members were secreted as proteoglycans with various types of glycosaminoglycan chains, *i.e.* chondroitin/dermatan sulfate (CS/DS) or keratan sulfate (10), we next determined whether NPN is secreted in the extracellular space as predicted by the PSORT II program and post-translationally modified. As shown in Fig. 5, NPN was detected only in the cultured medium fraction but not in the cell lysate, demonstrating that NPN is a secreted protein (Fig. 5, *lanes 3* and *6*). The treatment with chondroitinase ABC or endo-β-galactosidase did not change the migration position of the NPN band on the gel, indicating the absence of glycosaminoglycan chains in NPN (data not shown). However, when treated with *N*-glycosidase F, the NPN band was shifted from ~80 to ~66 kDa (Fig. 5, *lane 4*) confirming the presence of *N*-glycosylation in NPN as the amino acid sequence suggested (Fig. 1*A*).

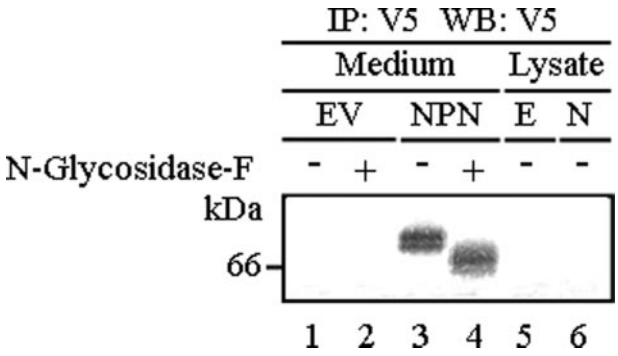

FIGURE 5. **NPN is a secreted glycoprotein.** The 293 cells were transfected with either an empty vector (*EV* or *E*) or pcDNA3.1-NPN-V5/His vector (*NPN* or *N*). After the cultured medium (*Medium*) or cell lysate (*Lysate*) was collected, the samples were immunoprecipitated (*IP*) with anti-V5 antibody (*V5*). The immunocomplex was treated with or without *N*-glycosidase F and detected by Western blotting (*WB*) using anti-V5 antibody. Markers of molecular mass are shown on the *left*. Note that NPN was detected only in the cultured medium fraction and not in the cell lysate, and the NPN band was shifted upon *N*-glycosidase F treatment.

NPN Inhibits TGF-β/Smad Signaling—It has been reported that several SLRP members, including DCN, interact with a number of growth factors such as TGF-β (22, 23), platelet-derived growth factor (30), and insulin-like growth factor-1 (31), and modulate their activities. Because we have identified the NPN gene based on the structural similarity to DCN, we investigated the possible regulatory function of NPN in TGF-β signaling. First, the effects of NPN on TGF-β-responsive luciferase promoter (3TP) activity were analyzed by overexpression or exogenous addition of NPN. As shown in Fig. 6*A*, overexpression of NPN inhibited 3TP promoter activity in 293 cells, and moreover, as shown in Fig. 6*B*, exogenous addition of NPN protein inhibited the activity in a dose-dependent manner. Second, the effects of NPN on Smad3 phosphorylation were analyzed by TGF-β stimulation with or without NPN (Fig. 6*C*) in 293 cells. Smad3 is a direct substrate of TGF-β receptors and is known to be phosphorylated upon TGF-β stimulation. As shown in Fig. 6*C*, NPN clearly down-regulated the Smad3 phosphorylation, indicating that NPN may function as an endogenous inhibitor of the TGF-β/Smad3 signaling pathway, upstream of Smad3 phosphorylation.

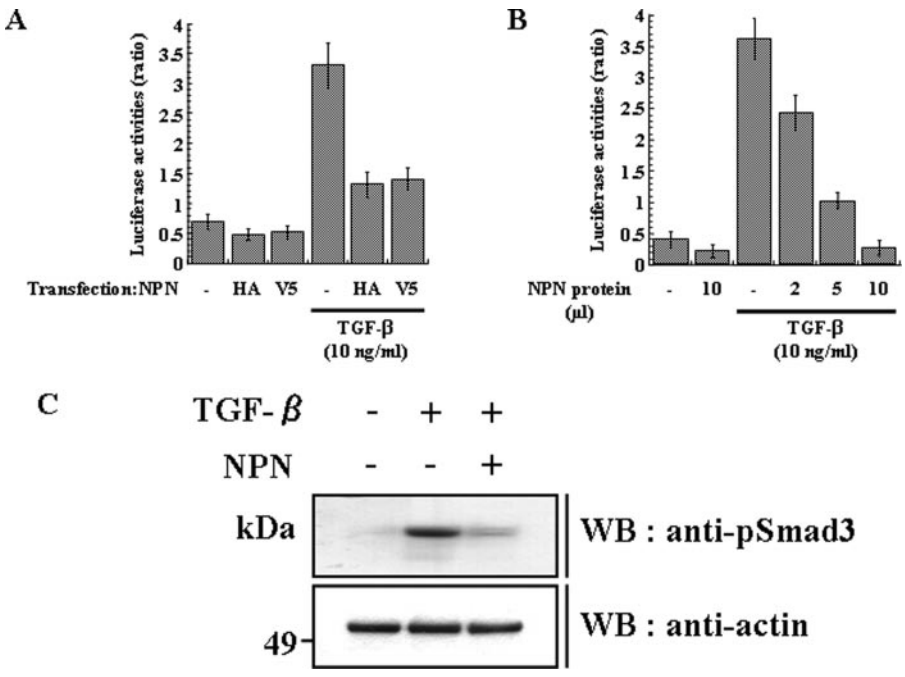

FIGURE 6. **NPN inhibits TGF-β/Smad signaling.** *A,* overexpression of NPN inhibits TGF-β-responsive luciferase activity. The 293 cells were transfected with an empty vector (−), pcDNA3-NPN-HA vector (*HA*), or pcDNA3.1-NPN-V5/His vector (*V5*) together with 3TP luciferase reporter plasmid and pRL-TK vectors. Cells were treated with 10 ng/ml human TGF-β1, and the luciferase activities in the cell lysates were measured. The values indicated represent normalized luciferase activities and are shown as mean ± S.D. based on assays done in triplicate. *B,* the addition of NPN protein inhibits TGF-β-responsive luciferase activity in a dose-dependent manner. The 293 cells were transfected with 3TP luciferase reporter plasmid and pRL-TK vectors and treated with 10 ng/ml human TGF-β1 and/or purified NPN-V5/His fusion protein (~50 ng/μl) as indicated. The luciferase activities were determined in the same manner as in *A*. *C,* NPN inhibits Smad3 phosphorylation induced by TGF-β. The 293 cells were treated with human TGF-β1 with or without purified NPN-V5/His fusion protein, and Western blotting (*WB*) was performed using anti-phospho-Smad3 antibody (anti-pSmad3). Equal protein loading was confirmed using anti-actin antibody.

DISCUSSION

Here we have reported identification and partial characterization of a new member of the SLRP family, NPN. It was identified by employing a bioinformatics approach based on its structural similarity to DCN. DCN, together with biglycan and asporin, is a member of class I SLRP subfamily; they all have eight exons in each gene, identical numbers of interspaced amino acids in the N-terminal cysteine cluster (CX_3CXCX_6C), and 10 LRRs in each core protein. Both DCN and biglycan, but not asporin, usually carry CS or DS glycosaminoglycan chain(s). In comparison with these characteristics of class I molecules, NPN has several distinct features; its gene has three exons, and the protein contains uniquely interspaced amino acids (CX_3CXCX_7C) in the N terminus (residues 21–35) and has 17 LRRs as shown in Fig. 1. In extracellular

proteins, LRR motifs are often flanked by cysteine clusters at both N- and C-terminal domains. The most common C-terminal flanking domain of SLRP members contains two cysteine residues (5); however, NPN has four cysteine residues (Fig. 1*A*, indicated by *double underlines*). In addition, class I SLRP members typically contain a propeptide that may function as a recognition sequence for xylosyltransferase that catalyzes the initial step of the biosynthesis of CS or DS glycosaminoglycan chains (32). However, NPN contains neither this conserved propeptide region nor serine-glycine (SG) sequence required for the *O*-linked glycosaminoglycan attachment. Therefore, NPN is likely not a proteoglycan but a glycoprotein (Fig. 5). According to NetNGlyc 1.0 Server program, the potential for glycosylation for all five asparagine residues in NPN was indeed above threshold (= 0.5) (amino acid 66 NFT 68; potential 0.6848, 88 NDT 90; potential 0.5676, 256 NLS 258; potential 0.6271, 278 NLT 280; potential 0.6336, 428 NCT 430; and potential 0.5281, respectively). Some of the SLRP members, *e.g.* asporin (33), osteoglycin (34), tsukushi (35), and podocan (36), are also known to be glycoproteins but not proteoglycans.

Another unique motif found in NPN is a polyacidic tail (DDDDDDYEID) at the C terminus. The tyrosine residue in this sequence is likely sulfated, because it resides next to acidic amino acids (37). The computational prediction using a Sulfinator program (38) also supports this notion (*E* value) (52). Therefore, an apparent molecular weight of NPN that is higher than the expected value (~58 kDa) (Figs. 3 and 5) is likely because of those extensive post-translational modifications.

In our attempt to identify NPN homologs among different species, putative NPN gene orthologs were found in pig (EST sequence number BE015058.1), dog (NCBI reference sequence number XM_541218), rat (NCBI reference sequence number XM_228174), and chicken (NCBI reference sequence number XM_426175), and interestingly, those are only conserved among higher animals. In addition, we cloned and sequenced a dog ortholog of NPN (GenBank™ accession number; DQ233647) using the dog kidney cDNA (BioChain Institute, Inc., Hayward, CA), and we found that the dog ortholog possesses a gene structure similar to that of mouse. At this point, it is not clear if the human counterpart of NPN gene exists. Although similar nucleotide sequences to mouse exon 2 and exon 3 were identified (GenBank™ accession number AL589939) in the human genomic cDNA library, exon 1 of human was not identified. The possible reasons are as follows: 1) the exon 1 of the human counterpart may have lesser homology with that of other animals, which makes the computational search difficult; and 2) during evolution, this gene might have become a pseudogene, accumulating mutations such as frameshifts, in-frame stop codons, or interspersed repeats in the original protein-coding sequence (39). The latter is less likely because the NPN gene appears to be well conserved among higher animals as we identified NPN genes in both mouse and dog. The search conditions may need to be modified to identify human NPN.

In the process of renal fibrosis, the trans-differentiation process referred to as the epithelial-mesenchymal transition (EMT), a process whereby epithelial cells lose cell adhesion, and the cell layers lose polarity and cell-cell contacts, is one of the essential mechanisms. TGF-β is a well characterized inducer of EMT, and it has been shown that this transition relies on Smad3-dependent transcription (40). It has been generally accepted that TGF-β, especially TGF-β1 isoform, is a predominant cytokine that causes renal fibrosis and plays an important role in the pathological accumulation of extracellular matrix proteins and degradation leading to kidney dysfunction (41). Interestingly, a potential regulatory function of DCN in the progression of renal fibrosis has been suggested. It has been demonstrated that the administration of DCN *in vivo* can antagonize the action of TGF-β on the accumulation of pathological matrix proteins in experimental kidney disease (42). However, DCN has been shown to be present in many tissues and organs such as heart, lung, liver, kidney, spleen, bone, and skin (43) and thus not specific to kidney. The ability of NPN to inhibit the TGF-β/Smad3 signaling pathway raises the possibility that NPN might be another regulatory protein responsible for converting EMT activities by TGF-β and controlling matrix accumulation in kidney. Interestingly, the transformation of mesenchyme to epithelium (MET), the reverse of EMT, occurs during kidney embryonic development. The cardinal feature of kidney development is the formation of epithelial tubules from nonepithelial mesenchymal cells. This conversion of cell type, MET, is controlled by factors secreted from the ureteric bud (29, 44, 45) at around embryonic day 10.5 to 11 in the mouse, and these epithelial inducers have been purified from ureteric bud cell lines (46) and show EMT converting activities in development and in cell culture (47). In this study, we showed that NPN is expressed in adult kidney. Moreover, NPN is up-regulated in 11-day-old embryo (Fig. 2*B*), a critical time for MET, suggesting its importance in kidney development. It would be of interest to investigate whether or not NPN is one of the endogenous epithelial inducers secreted by the ureteric bud.

TGF-β is known as a multifunctional growth factor with potential effects on growth, differentiation, extracellular matrix accumulation, and the immune system. In kidney, it is known that TGF-β contributes to renal fibrosis (48). NPN protein in adult mice kidney was mainly observed in distal tubules and collecting ducts (Fig. 4, *A* and *C*), indicating those cells synthesize and/or uptake NPN protein. In particular, the expression of NPN found in distal nephron is intriguing (Fig. 4). Fibrotic change in this area is common in chronic renal disease, and the pathology in the interstitium correlated with renal function. Therefore, NPN, as a TGF-β signaling inhibitor, may serve as an anti-fibrotic function.

At this point, it is still unclear how NPN inhibits TGF-β signaling. TGF-β is synthesized as a homodimeric proprotein, and dimeric propeptide is intracellularly cleaved. TGF-β propeptide, called LAP, has high affinity to mature TGF-β, and this tight complex is secreted together with latent TGF-β-binding protein(s) as a large molecular weight complex (49). Therefore, the dissociation from this complex is a central regulatory mechanism for the activation of TGF-β. Because the data demonstrated that NPN is a secreted protein (Fig. 5), the inhibitory effect(s) is likely through the extracellular interaction with the following: 1) mature TGF-β to inhibit the ligand-receptor(s) complex; 2) LAP and/or latent TGF-β-binding proteins to form a complex to inhibit the dissociation of mature TGF-β; and/or 3) TGF-β type I and/or type II receptor to block the binding of

mature TGF-β to its receptors. As it has been proposed that DCN and other SLRP members modulate the activities of TGF-β superfamily, including bone morphogenetic proteins (34, 35, 50), the results in this study further underscore critical roles of SLRP members in controlling TGF-β superfamily signaling.

Given that the predominant expression of NPN is in kidney and that it can inhibit the TGF-β/Smad3 signaling pathway, NPN could be an effective target molecule to prevent renal fibrosis. Thus, further studies on the mechanisms by which NPN inhibits TGF-β activities may potentially lead to the development of a strategy for the treatment of this disorder.

Acknowledgment—We thank Dr. Hidenori Ichijo for providing vectors.

REFERENCES

1. Bell, J. K., Mullen, G. E., Leifer, C. A., Mazzoni, A., Davies, D. R., and Segal, D. M. (2003) *Trends Immunol.* **24,** 528–533
2. Hocking, A. M., Shinomura, T., and McQuillan, D. J. (1998) *Matrix Biol.* **17,** 1–19
3. Inohara, N., and Nunez, G. (2003) *Nat. Rev. Immunol.* **3,** 371–382
4. Evdokimov, A. G., Anderson, D. E., Routzahn, K. M., and Waugh, D. S. (2001) *J. Mol. Biol.* **312,** 807–821
5. Kobe, B., and Kajava, A. V. (2001) *Curr. Opin. Struct. Biol.* **11,** 725–732
6. Wu, H., Maciejewski, M. W., Marintchev, A., Benashski, S. E., Mullen, G. P., and King, S. M. (2000) *Nat. Struct. Biol.* **7,** 575–579
7. Weber, I. T., Harrison, R. W., and Iozzo, R. V. (1996) *J. Biol. Chem.* **271,** 31767–31770
8. Scott, J. E. (1996) *Biochemistry* **35,** 8795–8799
9. Scott, P. G., McEwan, P. A., Dodd, C. M., Bergmann, E. M., Bishop, P. N., and Bella, J. (2004) *Proc. Natl. Acad. Sci. U. S. A.* **101,** 15633–15638
10. Iozzo, R. V. (1998) *Annu. Rev. Biochem.* **67,** 609–652
11. Iozzo, R. V. (1997) *Crit. Rev. Biochem. Mol. Biol.* **32,** 141–174
12. Iozzo, R. V. (1999) *J. Biol. Chem.* **274,** 18843–18846
13. Keene, D. R., San Antonio, J. D., Mayne, R., McQuillan, D. J., Sarris, G., Santoro, S. A., and Iozzo, R. V. (2000) *J. Biol. Chem.* **275,** 21801–21804
14. Kresse, H., Liszio, C., Schonherr, E., and Fisher, L. W. (1997) *J. Biol. Chem.* **272,** 18404–18410
15. Schonherr, E., Hausser, H., Beavan, L., and Kresse, H. (1995) *J. Biol. Chem.* **270,** 8877–8883
16. Svensson, L., Heinegard, D., and Oldberg, A. (1995) *J. Biol. Chem.* **270,** 20712–20716
17. Tenni, R., Viola, M., Welser, F., Sini, P., Giudici, C., Rossi, A., and Tira, M. E. (2002) *Eur. J. Biochem.* **269,** 1428–1437
18. Sini, P., Denti, A., Tira, M. E., and Balduini, C. (1997) *Glycoconj. J.* **14,** 871–874
19. Vogel, K. G., Paulsson, M., and Heinegard, D. (1984) *Biochem. J.* **223,** 587–597
20. Reed, C. C., Gauldie, J., and Iozzo, R. V. (2002) *Oncogene* **21,** 3688–3695
21. Santra, M., Eichstetter, I., and Iozzo, R. V. (2000) *J. Biol. Chem.* **275,** 35153–35161
22. Hildebrand, A., Romaris, M., Rasmussen, L. M., Heinegard, D., Twardzik, D. R., Border, W. A., and Ruoslahti, E. (1994) *Biochem. J.* **302,** 527–534
23. Takeuchi, Y., Kodama, Y., and Matsumoto, T. (1994) *J. Biol. Chem.* **269,** 32634–32638
24. Tasheva, E. S., Klocke, B., and Conrad, G. W. (2004) *Mol. Vis.* **10,** 758–772
25. Atsawasuwan, P., Mochida, Y., Parisuthiman, D., and Yamauchi, M. (2005) *Biochem. Biophys. Res. Commun.* **327,** 1042–1046
26. Kobe, B., and Deisenhofer, J. (1994) *Trends Biochem. Sci.* **19,** 415–421
27. Matsushima, N., Ohyanagi, T., Tanaka, T., and Kretsinger, R. H. (2000) *Proteins* **38,** 210–225
28. Thompson, J. D., Gibson, T. J., Plewniak, F., Jeanmougin, F., and Higgins, D. G. (1997) *Nucleic Acids Res.* **25,** 4876–4882
29. Vainio, S., and Lin, Y. (2002) *Nat. Rev. Genet.* **3,** 533–543
30. Nili, N., Cheema, A. N., Giordano, F. J., Barolet, A. W., Babaei, S., Hickey, R., Eskandarian, M. R., Smeets, M., Butany, J., Pasterkamp, G., and Strauss, B. H. (2003) *Am. J. Pathol.* **163,** 869–878
31. Schonherr, E., Sunderkotter, C., Iozzo, R. V., and Schaefer, L. (2005) *J. Biol. Chem.* **280,** 15767–15772
32. Wilson, I. B. (2004) *Cell. Mol. Life Sci.* **61,** 794–809
33. Lorenzo, P., Aspberg, A., Onnerfjord, P., Bayliss, M. T., Neame, P. J., and Heinegard, D. (2001) *J. Biol. Chem.* **276,** 12201–12211
34. Chen, X. D., Fisher, L. W., Robey, P. G., and Young, M. F. (2004) *FASEB J.* **18,** 948–958
35. Ohta, K., Lupo, G., Kuriyama, S., Keynes, R., Holt, C. E., Harris, W. A., Tanaka, H., and Ohnuma, S. (2004) *Dev. Cell* **7,** 347–358
36. Shimizu-Hirota, R., Sasamura, H., Kuroda, M., Kobayashi, E., and Saruta, T. (2004) *FEBS Lett.* **563,** 69–74
37. Onnerfjord, P., Heathfield, T. F., and Heinegard, D. (2004) *J. Biol. Chem.* **279,** 26–33
38. Monigatti, F., Gasteiger, E., Bairoch, A., and Jung, E. (2002) *Bioinformatics* (*Oxf.*) **18,** 769–770
39. Zhang, Z., and Gerstein, M. (2004) *Curr. Opin. Genet. Dev.* **14,** 328–335
40. Zeisberg, M., Hanai, J., Sugimoto, H., Mammoto, T., Charytan, D., Strutz, F., and Kalluri, R. (2003) *Nat. Med.* **9,** 964–968
41. Yu, L., Border, W. A., Huang, Y., and Noble, N. A. (2003) *Kidney Int.* **64,** 844–856
42. Border, W. A., Noble, N. A., Yamamoto, T., Harper, J. R., Yamaguchi, Y., Pierschbacher, M. D., and Ruoslahti, E. (1992) *Nature* **360,** 361–364
43. Scholzen, T., Solursh, M., Suzuki, S., Reiter, R., Morgan, J. L., Buchberg, A. M., Siracusa, L. D., and Iozzo, R. V. (1994) *J. Biol. Chem.* **269,** 28270–28281
44. Barasch, J., Yang, J., Ware, C. B., Taga, T., Yoshida, K., Erdjument-Bromage, H., Tempst, P., Parravicini, E., Malach, S., Aranoff, T., and Oliver, J. A. (1999) *Cell* **99,** 377–386
45. Plisov, S. Y., Yoshino, K., Dove, L. F., Higinbotham, K. G., Rubin, J. S., and Perantoni, A. O. (2001) *Development* (*Camb.*) **128,** 1045–1057
46. Barasch, J., Pressler, L., Connor, J., and Malik, A. (1996) *Am. J. Physiol.* **271,** F50–F61
47. Barasch, J. (2001) *Curr. Opin. Nephrol. Hypertens.* **10,** 429–436
48. Border, W. A., and Noble, N. A. (1994) *N. Engl. J. Med.* **331,** 1286–1292
49. Miyazono, K., Olofsson, A., Colosetti, P., and Heldin, C. H. (1991) *EMBO J.* **10,** 1091–1101
50. Kizawa, H., Kou, I., Iida, A., Sudo, A., Miyamoto, Y., Fukuda, A., Mabuchi, A., Kotani, A., Kawakami, A., Yamamoto, S., Uchida, A., Nakamura, K., Notoya, K., Nakamura, Y., and Ikegawa, S. (2005) *Nat. Genet.* **37,** 138–144